DOI:10.11817/j.issn.1672-7347.2022.210800

MiR-1-3p通过靶向FZD7增强卵巢癌细胞对铁死亡的敏感性

章迪[1]，屈斌[2]，胡彬[3]，曹可欣[4]，沈浩明[2]

（1. 中南大学湘雅三医院检验科，长沙 410013；2. 中南大学湘雅医学院附属肿瘤医院，湖南省肿瘤医院检验科，长沙 410013；3. 中南大学湘雅医学院附属肿瘤医院，湖南省肿瘤医院妇瘤二科，长沙 410013；4. 中南大学湘雅医学院医学检验系，长沙 410013）

[摘 要] 目的：卷曲蛋白7(Frizzled 7，FZD7)在多种癌症中异常表达和激活。在卵巢癌中，FZD7的过表达可降低铂耐药性卵巢癌细胞对铁死亡的敏感性，从而使癌细胞存活，但FZD7是否抑制卵巢癌细胞铁死亡及其相关机制尚未被阐明。本研究通过探究FZD7及其上游调控因子miR-1-3p对卵巢癌细胞铁死亡的影响，旨在明确miR-1-3p及FZD7参与卵巢癌细胞铁死亡的分子机制。**方法：**以人卵巢癌细胞系HO8910和SKOV3为研究对象，第1部分实验将空白质粒和FZD7过表达质粒分别转染人卵巢癌细胞；第2，3部分实验将miR-1-3p模拟物阴性对照、miR-1-3p模拟物、miR-1-3p抑制剂阴性对照和miR-1-3p抑制剂分别转染人卵巢癌细胞；第4部分实验将miR-1-3p模拟物、miR-1-3p模拟物+FZD7过表达质粒分别转染人卵巢癌细胞，另设正常培养的对照组。采用铁死亡诱导剂Erastin或RSL3分别孵育经不同处理后的人卵巢癌细胞构建人卵巢癌细胞铁死亡模型。使用real-time RT-PCR检测*FZD7*和*miR-1-3p*的mRNA表达水平，蛋白质印迹法检测FZD7的蛋白质表达水平，CCK-8实验检测细胞活力，脂质过氧化比色测定试剂盒检测细胞内MDA水平，铁检测试剂盒检测细胞内Fe^{2+}水平，双荧光素酶实验检测miR-1-3p和FZD7的靶向关系。**结果：**FZD7的过表达提高经Erastin或RSL3处理的人卵巢癌细胞系HO8910或SKOV3细胞的活力(P<0.05、P<0.01或P<0.001)，并降低细胞内MDA的水平(P<0.01)。FZD7是miR-1-3p的直接靶点，miR-1-3p通过与FZD7的3'非翻译区(3'-untranslated region，3'UTR)位点结合，抑制FZD7的表达(P<0.01)。MiR-1-3p模拟物降低经Erastin或RSL3处理的人卵巢癌细胞系HO8910或SKOV3细胞的活力(P<0.05、P<0.01或P<0.001)，提高细胞内MDA的水平(P<0.01)，而miR-1-3p抑制剂则显著提高经Erastin或RSL3处理的人卵巢癌细胞系HO8910或SKOV3细胞的活力(P<0.05、P<0.01或P<0.001)，降低细胞内MDA的水平(P<0.01)。MiR-1-3p模拟物增强人卵巢癌细胞对Erastin或RSL3诱导细胞铁死亡敏感性的作用可以被FZD7的过表达所取消(P<0.05或P<0.01)。**结论：**MiR-1-3p靶向FZD7增强卵巢癌细胞对铁死亡的敏感性。

[关键词] 卵巢癌；铁死亡；miR-1-3p；卷曲蛋白7

MiR-1-3p enhances the sensitivity of ovarian cancer cells to ferroptosis by targeting FZD7

ZHANG Di[1], QU Bin[2], HU Bin[3], CAO Kexin[4], SHEN Haoming[2]

收稿日期(Date of reception)：2021-12-31

第一作者(First author)：章迪，Email: 10416475@qq.com, ORCID: 0000-0002-7624-236X

通信作者(Corresponding author)：沈浩明，Email: shenhaoming@hnca.org.cn, ORCID: 0000-0001-8865-4508

基金项目(Foundation item)：湖南省自然科学基金(2021JJ70026)。This work was supported by the Natural Science Foundation of Hunan Province, China (2021JJ70026).

(1. Department of Laboratory Medicine, Third Xiangya Hospital, Central South University, Changsha 410013; 2. Department of Laboratory Medicine, Hunan Cancer Hospital & Affiliated Cancer Hospital of Xiangya School of Medicine, Central South University, Changsha 410013; 3. Second Department of Gynecologic Oncology, Hunan Cancer Hospital & Affiliated Cancer Hospital of Xiangya School of Medicine, Central South University, Changsha 410013; 4. Department of Laboratory Medicine, Xiangya School of Medicine, Central South University, Changsha 410013, China)

ABSTRACT

Objective: Frizzled 7 (FZD7) is abnormally expressed and activated in a variety of cancers. In ovarian cancer, overexpression of FZD7 reduces the sensitivity of platinum-resistant ovarian cancer cells to ferroptosis, thereby allowing cancer cells to survive. However, whether FZD7 inhibits ferroptosis in ovarian cancer cells and its mechanisms are remain unclear. This study aims to explore the effects of FZD7 and its upstream regulator miR-1-3p on ferroptosis in ovarian cancer cells are evaluated to clarify the molecular mechanism for miR-1-3p and FZD7's involvement in ferroptosis in ovarian cancer cells.

Methods: Human ovarian cancer cell lines HO8910 and SKOV3 were used as the research subjects. In the first part of the experiment, human ovarian cancer cells were transfected with blank plasmid and FZD7 overexpression plasmid, respectively; in the second and third parts, human ovarian cancer cells were transfected with miR-1-3p mimics negative control, miR-1-3p mimics, miR-1-3p inhibitors negative control, and miR-1-3p inhibitors, respectively; in the fourth part of the experiment, human ovarian cancer cells were transfected with miR-1-3p mimics and miR-1-3p mimics+FZD7 overexpression plasmid, respectively, and normal cultured cells were set as the control group. The human ovarian cancer cell ferroptosis model was established by incubating human ovarian cancer cells with different treatments with ferroptosis inducer Erastin or RSL3. Real-time RT-PCR was used to detect the mRNA expression levels of *FZD7* and *miR-1-3p*; Western blotting was used to detect the protein expression levels of FZD7; CCK-8 assay was used to detect the cell viability; lipid peroxidation colorimetric assay kit was used to detect the level of intracellular MDA; and iron assay kit was used to detect the level of intracellular Fe^{2+}. Dual-luciferase assay was used to detect the targeting relationship between miR-1-3p and FZD7.

Results: Overexpression of FZD7 increased the cell viability of human ovarian cancer cell lines HO8910 or SKOV3 (P<0.05, P<0.01, or P<0.001) and decreased the intracellular MDA levels (P<0.01) in Erastin-treated or RSL3-treated ovarian cancer cells. FZD7 was a direct target of miR-1-3p, which inhibited the expression of FZD7 (P<0.01) by binding to the 3'-untranslated region (3'UTR) site of FZD7. MiR-1-3p mimics decreased the cell viability of human ovarian cancer cell lines HO8910 or SKOV3 (P<0.05, P<0.01, or P<0.001) and increased the intracellular MDA levels (P<0.01) in Erastin-treated or RSL3-treated ovarian cancer cells; while miR-1-3p inhibitors significantly increased the cell viability of human ovarian cancer cell lines HO8910 or SKOV3 (P<0.05, P<0.01, or P<0.001) and decreased the intracellular MDA levels (P<0.01) in Erastin-treated or RSL3-treated ovarian cancer cells. The effect of miR-1-3p mimics on enhancing the sensitivity of human ovarian cancer cells to Erastin-induced or RSL3-induced ferroptosis was abrogated by overexpression of FZD7(P<0.05 or P<0.01).

Conclusion: MiR-1-3p enhances the sensitivity of ovarian cancer cells to ferroptosis by targeting FZD7.

KEY WORDS　ovarian cancer; ferroptosis; miR-1-3p; Frizzled 7

卵巢癌是致命的妇科癌症，也是导致女性癌症相关死亡的第五大原因[1]。卵巢癌早期无明显症状且缺乏有效的筛查手段，因此60%的卵巢癌患者在诊断时已是晚期，患者5年总生存率仅为29%[2]。虽然近几十年来外科治疗和化学治疗取得了巨大的进步，卵巢癌的病死率显著下降，但仍然很高[3]。因此深入了解卵巢癌的发生和发展机制，探寻新的有效治疗靶点具有重要意义。

卷曲蛋白7(Frizzled 7，FZD7)受体是FZD蛋白质家族受体之一，可介导经典和非经典Wnt信号转导[4]。FZD7的过表达可以导致Wnt/β-catenin信号通路过度激活，并促进胃癌发生[5]；可以取消miR-129-5p对乳腺癌细胞增殖、迁移、侵袭的抑制作用[6]。在卵巢癌组织过表达的FZD7通过Wnt信号通路促进卵巢癌的发生和发展[7-8]。最新的研究[9]发现：过表达的FZD7降低了铂耐药性卵巢癌细胞对铁死亡的敏感性，使癌细胞存活。铁死亡是一种铁和ROS依赖性细胞死亡途径，在形态学、生物化学和遗传学方面不同于细胞凋亡、坏死和自噬[10]。诱导卵巢癌细胞铁死亡可能是治疗卵巢癌的新思路[11-12]，但尚未有研究明确FZD7及其上游调控因子miR-1-3p是否可以影响卵巢癌细胞的铁死亡。因此，本研究通过体外细胞实验探究FZD7及其上游调控因子miR-1-3p对卵巢癌细胞铁死亡的影响，以期阐明miR-1-3p及FZD7参与卵巢癌细胞铁死亡的分子机制。

1 材料与方法

1.1 材料

人卵巢上皮细胞系HOSE，人卵巢癌细胞系HO8910、SKOV3，人胚肾细胞系293T均购自中国科学院；胎牛血清、RPMI 1640培养基、胰蛋白酶均购自美国Gibco公司；青霉素(100 U/mL)和链霉素(100 μg/mL)双抗购自美国HyClone公司；铁死亡诱导剂Erastin和RSL3均购自美国Cayman Chemical公司；Lipofectamine 2000购自美国Invitrogen公司；FZD7过表达/空白载体、miR-1-3p模拟物/模拟物阴性对照、miR-1-3p抑制剂/抑制剂阴性对照均购自中国苏州吉玛基因股份有限公司；RNeasy Mini试剂盒、miRNeasy Mini试剂盒均购自美国Qiagen公司；TaqMan miRNA检测试剂盒、PrimeScript RT试剂盒、蛋白质提取试剂盒均购自美国Thermo Fisher Scientific公司；FastStart Universal SYBR Green Master试剂盒购自德国Roche Diagnostics公司；BCA蛋白质含量检测试剂盒购自上海碧云天生物技术有限公司；PVDF膜购自美国Bio-Rad公司；FZD7抗体、GAPDH抗体、羊抗兔二抗、CCK-8试剂盒均购自英国Abcam公司；MDA比色测定试剂盒、铁测定试剂盒均购自美国Biovision公司。

1.2 方法

1.2.1 细胞培养和转染

人卵巢上皮细胞系HOSE、人卵巢癌细胞系HO8910或SKOV3采用含有10%胎牛血清和1%双抗的RPMI 1640培养基，置于37 ℃和5% CO_2培养箱中培养。待细胞密度达80%~90%时，用胰蛋白酶消化，传代培养或冻存。

构建空白质粒(Lenti-Empty)和过表达质粒(Lenti-FZD7)慢病毒表达载体，测序鉴定后使用Lipofectamine 2000转染293T细胞，48 h后收集上清液，获取慢病毒滤液。取对数生长期的HO8910或SKOV3细胞，在细胞密度达到80%时，分别用Lenti-Empty和Lenti-FZD7慢病毒滤液感染细胞，命名为Lenti-Empty组和Lenti-FZD7组。

在6孔板中培养HO8910或SKOV3细胞至细胞密度达85%时，使用Lipofectamine 2000将miR-1-3p模拟物阴性对照(Mimics NC组)、miR-1-3p模拟物(Mimics miR-1-3p组)、miR-1-3p抑制剂阴性对照(Inhibitors NC组)和miR-1-3p抑制剂(Inhibitors miR-1-3p组)转染细胞。6 h后，将培养基更换为含10%胎牛血清的RPMI 1640培养基。培养48 h后，进行实验分析。

在6孔板中培养HO8910或SKOV3细胞至细胞密度达85%时，使用Lipofectamine 2000将miR-1-3p模拟物(Mimics miR-1-3p组)、miR-1-3p模拟物和FZD7过表达质粒(Mimics miR-1-3p+Lenti-FZD7组)转染细胞，以不进行任何处理、正常培养的HO8910或SKOV3细胞为对照(Control组)。6 h后，将培养基更换为含10%胎牛血清的RPMI 1640培养基。培养48 h后，进行实验分析。

1.2.2 Real-time RT-PCR

根据RNeasy Mini和miRNeasy Mini试剂盒说明书，从细胞中提取总RNA和miRNA。使用TaqMan miRNA检测试剂盒、PrimeScript RT试剂盒、FastStart Universal SYBR Green Master试剂盒进行real-time RT-PCR，Applied Biosystems7900快速实时荧光定量PCR系统对*miR-1-3p*、*FZD7*的表达进行定量分析。实验重复3次。以*U6*为内参，计算*miR-1-3p* mRNA的相对表达量；以*β-actin*为内参，计算*FZD7* mRNA的相对表达量。采用$2^{-\Delta\Delta Ct}$方法计算目的基因的相对表达水平。引物序列见表1。

表1　PCR引物序列

Table 1　PCR primer sequences

Gene	Primer sequence (5'-3')	Size/bp
FZD7	Forward: TTATAGGCAAAGCAGCGCAAATC	23
	Reverse: CCTCTGGCTTAACGGTGTGTGA	22
β-actin	Forward: GGCTGTGCTATCCCTGTACG	20
	Reverse: AGGTAGTCAGTCAGGTCCCG	20
miR-1-3p	Forward: ACACTCCAGGTGGGTGGAATGT	22
	Reverse: CTCAACTGGTGTCGTGGAG	19
U6	Forward: CTCGCTTCGGCAGCACA	17
	Reverse: AACGCTTCACGAATTTGCGT	20

FZD7：Frizzled 7.

1.2.3 蛋白质印迹法

收集经处理后的人卵巢癌细胞，用PBS洗涤，加入适量细胞裂解液，置于低温高速离心机中，以12 000 r/min离心10 min，收集上清液至1.5 mL EP管中。采用蛋白质提取试剂盒提取总蛋白质。根据BCA蛋白质含量检测试剂盒说明书测定蛋白质浓度。取等量的蛋白质进行SDS-PAGE，随后转膜，并在室温下封闭0.5 h。将膜与一抗(FZD7稀释比例1∶3 000，GAPDH稀释比例1∶2 500) 于4 ℃下孵育过夜；然后将膜与羊抗兔二抗(稀释比例1∶2 500) 于室温下孵育90 min。采用ECL显色曝光，Image J软件分析目标条带的灰度值，并计算目标蛋白质的相对表达水平。

1.2.4 CCK-8实验

采用CCK-8试剂盒检测细胞活力。将各组人卵巢癌细胞接种到96孔板中，24 h后采用不同浓度的铁死亡诱导剂Erastin (0、2.5、5.0、7.5和10.0 μmol/L)或RSL3 (0、0.2、0.4、0.8和1.6 μmol/L)处理24 h；每孔加入10 μL CCK-8溶液，于37 ℃下孵育1~4 h；通过酶标仪测量450 nm处的吸光度值。实验重复3次。

1.2.5 MDA水平的测定

按照MDA测定试剂盒说明书进行操作。使用胰蛋白酶消化处理后的人卵巢癌细胞，以3 000 r/min离心10 min；用500 μL去离子水将沉淀重新悬浮，通过5次超声循环裂解细胞；加入1 mL TBA溶液(15%三氯乙酸、0.8%硫代巴比妥酸、0.25 mol/L盐酸)；将混合物在95 ℃加热15 min，以形成MDA-TBA加合物；通过分光光度计测量532 nm处的吸光度值，并计算MDA的水平。

1.2.6 Fe^{2+}水平的测定

通过铁测定试剂盒测定细胞中Fe^{2+}水平。将经处理后的人卵巢细胞按2×10^6 /mL的密度在4~10倍体积的铁测定缓冲液中快速均质化。随后，将细胞样品于4 ℃下离心(13 000 r/min) 10 min，以去除不溶性物质。将5 μL铁测定缓冲液添加到每个细胞样品中。使用水平振荡器将样品充分振荡混匀，于室温下避光孵育30 min。将100 μL铁探针添加到样品中，于室温下避光孵育60 min。在593 nm处测量吸光度值，并计算Fe^{2+}的水平。

1.2.7 双荧光素酶实验

通过生物信息学网站(https://www.targetscan.org/)预测miR-1-3p与FZD7的3'非翻译区(3'-untranslated region，3'UTR)区是否有结合位点。双荧光素酶报告分析用于检测miR-1-3p是否直接靶向FZD7。构建野生型FZD7-WT-3'UTR和突变型FZD7-MUT-3'UTR荧光素酶报告基因载体，将其分别与miR-1-3p模拟物(Mimics miR-1-3p组)或miR-1-3p模拟物阴性对照(Mimics NC组)共转染到人卵巢癌细胞系HO8910或SKOV3细胞中，然后接种于24孔细胞培养板中，培养48 h后，测定荧光素酶活性，计算相对荧光强度，并分析miR-1-3p与FZD7的3'UTR区是否直接结合。

1.3 统计学处理

采用SPSS 23.0软件分析数据。计量资料均采用均数±标准差($\bar{x}\pm s$)描述，两组间的均数比较采用t检验，两组以上的均数比较采用方差分析。P<0.05表示差异具有统计学意义。

2 结　果

2.1 FZD7抑制Erastin或RSL3诱导的卵巢癌细胞铁死亡

Real-time RT-PCR和蛋白质印迹法结果显示：与Lenti-Empty组相比，Lenti-FZD7组HO8910或SKOV3细胞内*FZD7*的mRNA和蛋白质相对表达水平均显著上调(均P<0.001；图1A，1B)。

CCK-8实验结果显示：经Erastin (0、2.5、5.0、7.5和10.0 μmol/L)或RSL3 (0、0.2、0.4、0.8和1.6 μmol/L)处理后，与Lenti-Empty组相比，Lenti-FZD7组HO8910或SKOV3细胞的活力均较高(P<0.05、P<

0.01或P<0.001；图1C)。

经Erastin (10.0 μmol/L)或RSL3 (1.6 μmol/L)处理后，与Lenti-Empty组相比，Lenti-FZD7组HO8910或SKOV3细胞内MDA水平均较低(均P<0.01，图1D)，但Fe^{2+}水平差异均无统计学意义(均P>0.05，图1E)。

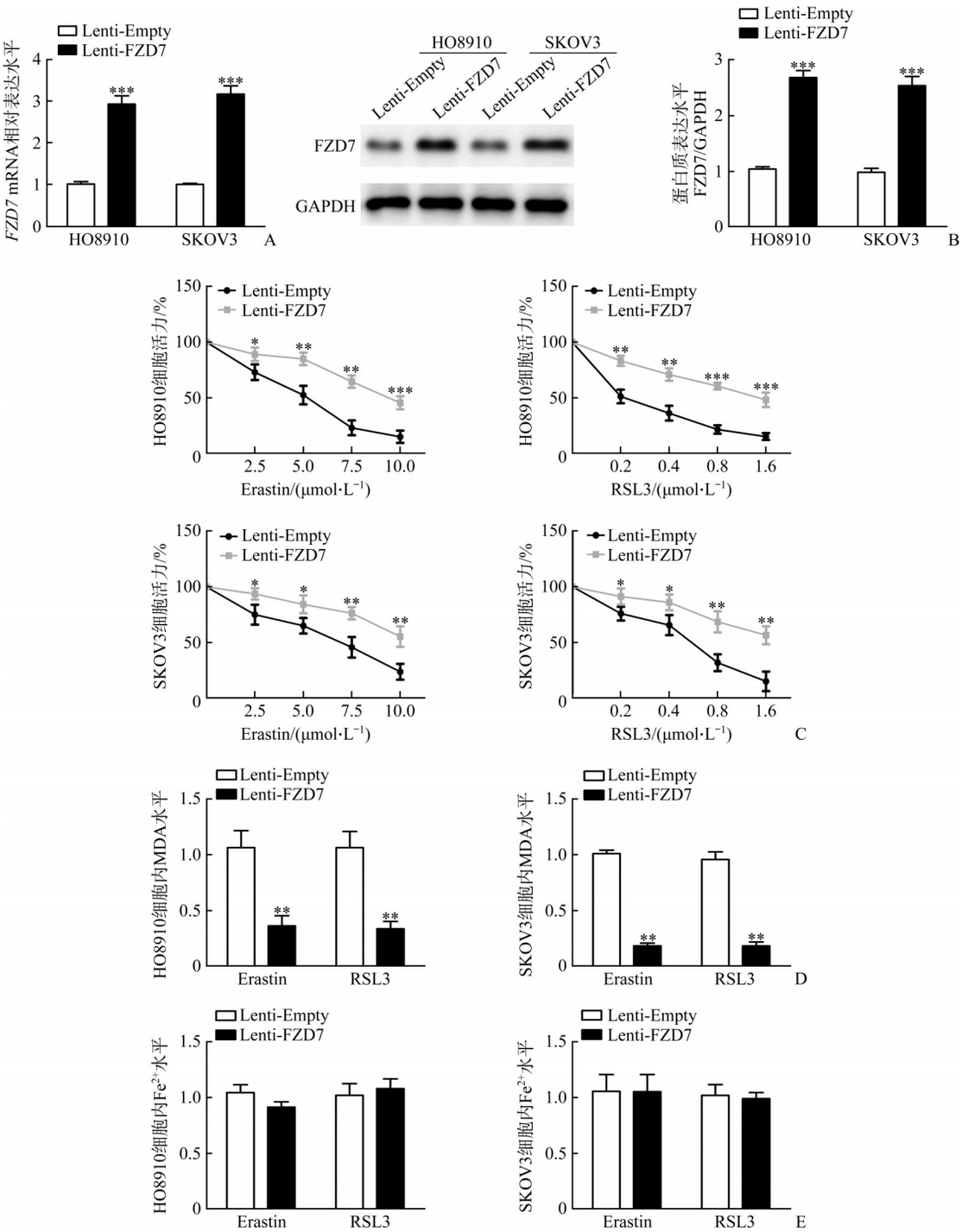

图1 FZD7抑制Erastin或RSL3诱导的卵巢癌细胞铁死亡

Figure 1 FZD7 inhibits Erastin-induced or RSL3-induced ferroptosis in ovarian cancer cells

A: mRNA relative expression levels of *FZD7* in HO8910 or SKOV3 cells; B: Protein expression levels of FZD7 detected by Western blotting in HO8910 or SKOV3 cells; C: Cell viability of HO8910 or SKOV3 cells treated with different concentrations of Erastin or RSL3; D: Intracellular MDA levels in HO8910 or SKOV3 cells treated with Erastin (10.0 μmol/L) or RSL3 (1.6 μmol/L); E: Intracellular Fe^{2+} levels in HO8910 or SKOV3 cells treated with Erastin (10.0 μmol/L) or RSL3 (1.6 μmol/L). *P<0.05, **P<0.01, ***P<0.001 vs the Lenti-Empty group. FZD7: Frizzled 7; HO8910 or SKVO3: Human ovarian cancer cells; Erastin or RSL3: Ferroptosis inducers.

2.2 FZD7是miR-1-3p的直接靶点

生物信息学网站预测结果显示：FZD7是miR-1-3p的潜在靶点，*FZD7* mRNA的3'UTR包含1个与miR-1-3p高度保守的结合位点(图2A)。

双荧光素酶实验结果显示：与Mimics NC组相比，Mimics miR-1-3p组HO8910或SKOV3细胞的FZD7野生型基因(FZD7-WT-3'UTR)报告的荧光素酶活性均显著降低(均*P*<0.001，图2B)，但2组之间FZD7突变型基因(FZD7-MUT-3'UTR)报告的荧光素酶活性差异均无统计学意义(均*P*>0.05，图2B)。

Real-time RT-PCR和蛋白质印迹法结果显示：与Mimics NC组相比，Mimics miR-1-3p组HO8910或SKOV3细胞内*FZD7*的mRNA和蛋白质相对表达水平均显著下调(均*P*<0.01；图2C，2D)；而与Inhibitors NC组相比，Inhibitors miR-1-3p组HO8910或SKOV3细胞内*FZD7*的mRNA和蛋白质相对表达水平均显著上调(均*P*<0.01；图2C，2D)。

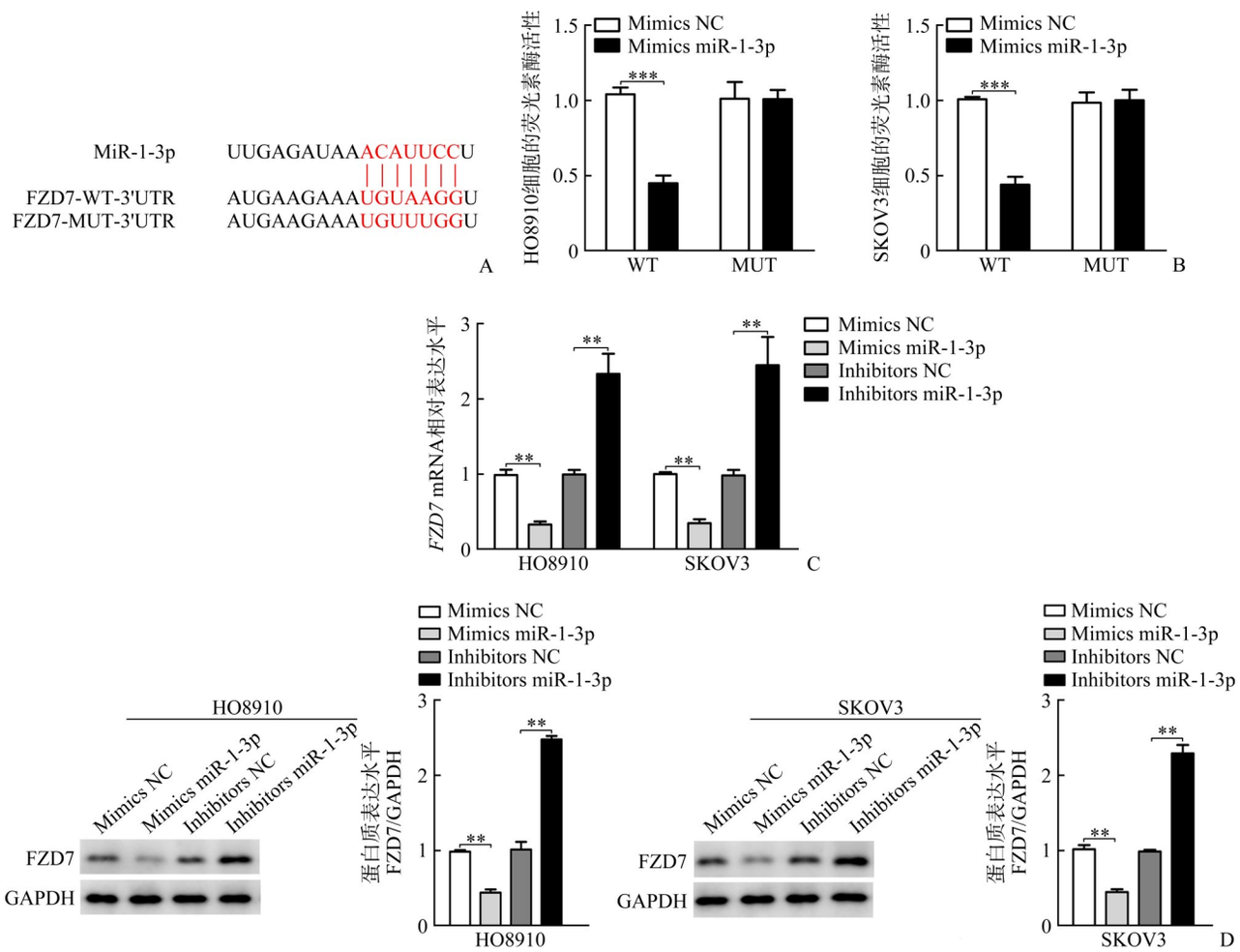

图2　FZD7是miR-1-3p的直接靶点

Figure 2　FZD7 is a direct target of miR-1-3p

A: Binding site map of *FZD7* and *miR-1-3p*; B: Results of dual luciferase assay in HO8910 or SKOV3 cells; C: mRNA relative expression levels of *FZD7* detected by real-time RT-PCR in HO8910 or SKOV3 cells; D: Protein expression levels of FZD7 detected by Western blotting in HO8910 or SKOV3 cells. ***P*<0.01, ****P*<0.001. FZD7: Frizzled 7; WT: Wild type; MUT: Mutant; 3'UTR: 3'-Untranslated region; HO8910 or SKVO3: Human ovarian cancer cells; NC: Negative control.

2.3 MiR-1-3p增加人卵巢癌细胞对Erastin或RSL3诱导的铁死亡的敏感性

Real-time RT-PCR结果显示：与HOSE细胞相比，HO8910或SKOV3细胞中*miR-1-3p*的mRNA相对表达水平均显著下调(均*P*<0.001，图3A)。在HO8910或SKOV3细胞中，与Mimics NC组相比，Mimics miR-1-3p组的*miR-1-3p*的相对表达水平均显著上调(均*P*<0.001，图3B)；而与Inhibitors NC组相

比，Inhibitors miR-1-3p组的*miR-1-3p*的mRNA相对表达水平均显著下调(均P<0.001，图3B)。

CCK-8实验结果显示：经Erastin (0、2.5、5.0、7.5和10.0 μmol/L)或RSL3 (0、0.2、0.4、0.8和1.6 μmol/L)处理后，与Mimics NC组相比，Mimics miR-1-3p组HO8910或SKOV3细胞的活力均较低(P<0.05、P<0.01或P<0.001，图3C)；而与Inhibitors NC组相比，Inhibitors miR-1-3p组HO8910或SKOV3细胞的活力均较高(P<0.05，P<0.01或P<0.001；图3C)。

经Erastin (10.0 μmol/L)或RSL3 (1.6 μmol/L)处理后，与Mimics NC组相比，Mimics miR-1-3p组HO8910或SKOV3细胞内MDA水平均较高(均P<0.01，图3D)；而与Inhibitors NC组相比，Inhibitors miR-1-3p组的HO8910或SKOV3细胞内MDA水平均较低(均P<0.01，图3D)。

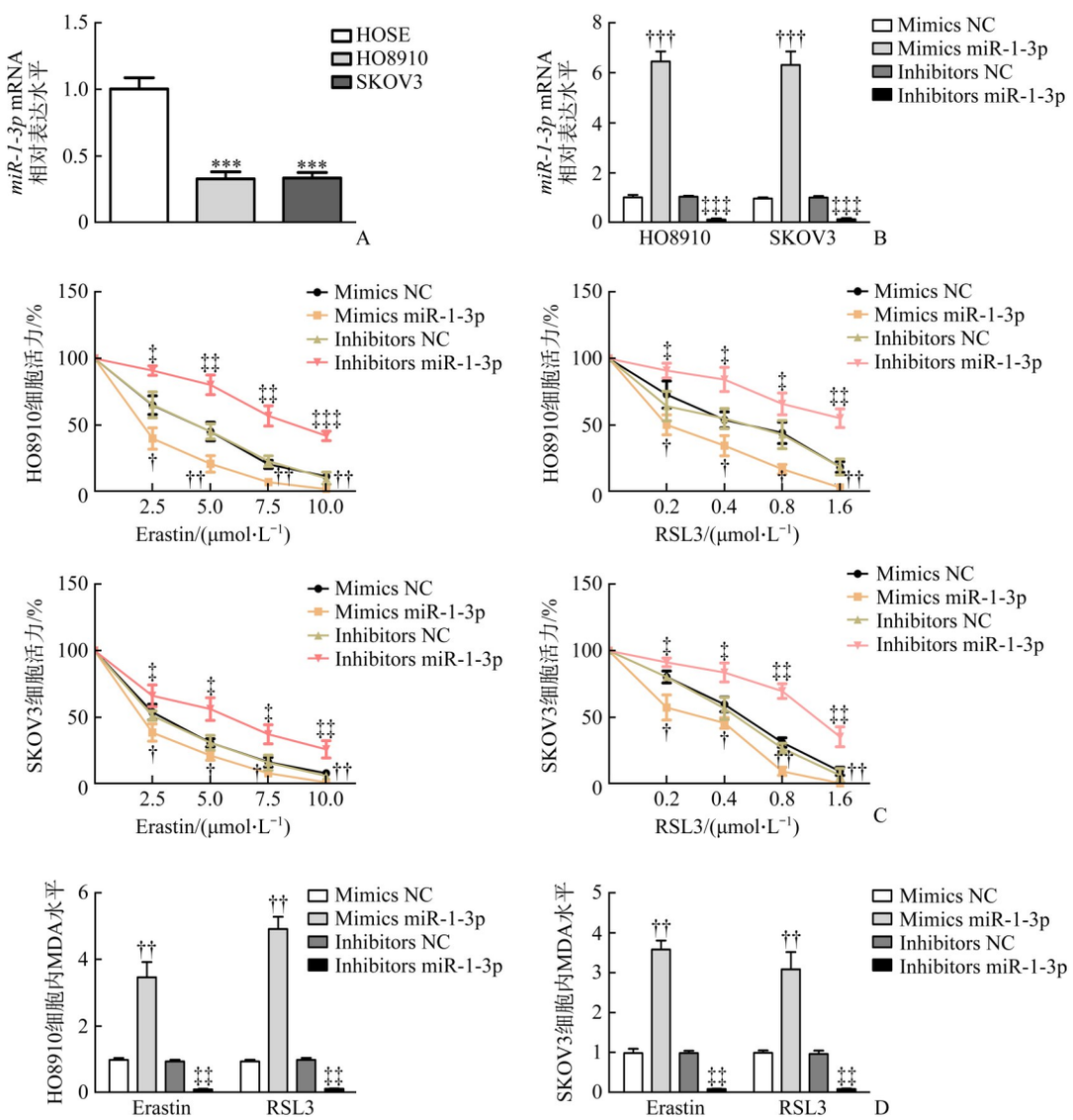

图3 MiR-1-3p增加人卵巢癌细胞对Erastin或RSL3诱导的铁死亡的敏感性

Figure 3 MiR-1-3p increases the sensitivity of human ovarian cancer cells to Erastin-induced or RSL3-induced ferroptosis

A: mRNA relative expression levels of *miR-1-3p* in HOSE, HO8910 or SKOV3 cells; B: mRNA relative expression levels of *miR-1-3p* in HO8910 or SKOV3 cells treated differently; C: Cell viability of HO8910 or SKOV3 cells treated with different concentrations of Erastin or RSL3; D: Intracellular MDA levels in HO8910 or SKOV3 cells treated with Erastin (10.0 μmol/L) or RSL3 (1.6 μmol/L). ***P<0.001 vs the HOSE group; †P<0.05, ††P<0.01,†††P<0.001 vs the Mimics NC group; ‡P<0.05, ‡‡P<0.01, ‡‡‡P<0.001 vs the Inhibitors NC group. HOSE: Human ovarian epithelial cells; HO8910 or SKVO3: Human ovarian cancer cells; Erastin or RSL3: Ferroptosis inducers; NC: Negative control.

2.4 MiR-1-3p削弱FZD7对卵巢癌细胞铁死亡的抑制

蛋白质印迹法结果显示：与Control组相比，Mimics miR-1-3p组HO8910或SKOV3细胞的FZD7的蛋白质相对表达水平均显著下调(均P<0.01)，Mimics miR-1-3p+Lenti-FZD7组HO8910或SKOV3细胞的FZD7的蛋白质相对表达水平差异均无统计学意义(均P>0.05，图4A)。说明上调的miR-1-3p显著抑制FZD7的表达，但这种抑制作用被FZD7的过表达所取消。

CCK-8实验结果显示：经Erastin (0、2.5、5.0、7.5和10.0 μmol/L)或RSL3 (0、0.2、0.4、0.8和1.6 μmol/L)处理后，与Control组相比，Mimics miR-1-3p组HO8910或SKOV3细胞的活力均显著降低(均P<0.05或P<0.01)，而Mimics miR-1-3p+Lenti-FZD7组HO8910或SKOV3细胞的活力差异均无统计学意义(均P>0.05，图4B)。

经Erastin (10.0 μmol/L)或RSL3 (1.6 μmol/L)处理后，与Control组相比，Mimics miR-1-3p组HO8910或SKOV3细胞内MDA水平均较高(均P<0.01)，而Mimics miR-1-3p+Lenti-FZD7组的HO8910或SKOV3细胞内MDA水平差异均无统计学意义(均P>0.05，图4C)。

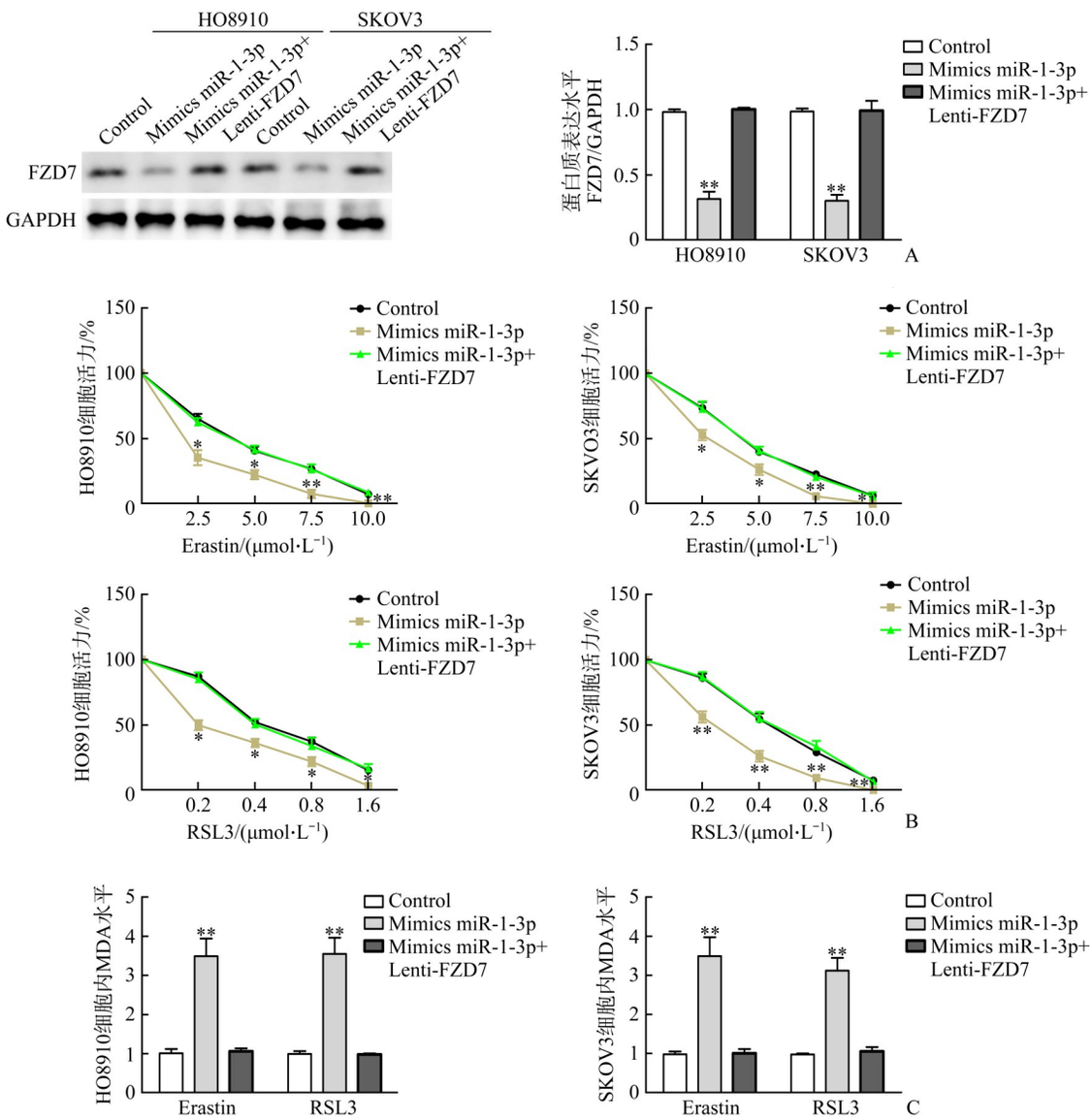

图4　MiR-1-3p削弱FZD7对卵巢癌细胞铁死亡的抑制

Figure 4　MiR-1-3p attenuates FZD7-mediated suppression for ferroptosis in ovarian cancer cells

A: Protein expression levels of FZD7 detected by Western blotting in HO8910 or SKOV3 cells with different treatments; B: Cell viability of HO8910 or SKOV3 cells with different concentrations of Erastin or RSL3; C: Intracellular MDA levels in HO8910 or SKOV3 cells treated with Erastin (10.0 μmol/L) or RSL3 (1.6 μmol/L). *P<0.05, **P<0.01 vs the Control group. FZD7: Frizzled 7; HO8910 or SKVO3: Human ovarian cancer cells; Erastin or RSL3: Ferroptosis inducers.

3 讨 论

铁死亡是一种铁依赖性细胞死亡途径，其特征是谷胱甘肽过氧化物酶4(glutathione peroxidase 4，GPX4)活性降低、脂质过氧化增加和线粒体损伤[13-14]。铁死亡对胃癌[15]、非小细胞肺癌[16]、胶质母细胞瘤[17]等多种肿瘤的发生和发展起抑制作用。近年，研究者们开始探究铁死亡在卵巢癌中的作用及其机制。Carbone等[11]研究发现：在胃癌中具有抗铁死亡的硬脂酰CoA去饱和酶1(stearoyl-CoA desaturase 1，SCD1)在卵巢癌组织中高表达，且SCD1抑制剂可以诱导卵巢癌细胞铁死亡，抑制肿瘤生长。Chan等[18]研究发现：MAP30(从苦瓜中提取的一种生物活性蛋白质)可以诱导细胞内Ca^{2+}浓度增加，从而通过细胞凋亡和铁死亡途径触发癌细胞死亡。上述研究结果表明铁死亡在卵巢癌中起抑癌因子的作用。因此以铁死亡为切入点，寻找治疗卵巢癌的方法，可能具有重要意义。但目前的研究对铁死亡参与卵巢癌发生和发展的分子机制尚未明确。

在卵巢癌组织中，过表达的FZD7通过上调GPX4的表达，降低铂耐药性卵巢癌细胞对铁死亡的敏感性[9]。本研究采用铁死亡诱导剂Erastin或RSL3处理经FZD7过表达慢病毒感染的人卵巢癌细胞系HO8910和SKOV3，观察其细胞活力、细胞内MDA和Fe^{2+}的水平，探究FZD7对卵巢癌细胞铁死亡的影响。结果显示：FZD7过表达可降低细胞内MDA的水平，抑制Erastin或RSL3诱导的卵巢癌细胞铁死亡。这表明FZD7能降低卵巢癌细胞及铂耐药性卵巢癌细胞对铁死亡的敏感性。

MiRNA是大约22个核苷酸的小型非编码RNA，可在转录后调节基因表达。MiRNA通过调控下游靶基因表达影响铁死亡：*miR-137*、*miR-9*和*miR-103a-3p*分别通过直接抑制代谢相关基因*SLC1A5*、*GOT1*和*GLS2*的表达来抑制癌细胞中Erastin诱导的铁死亡[19-20]；而*miR-214-3p*、*miR-489-3p*和*miR-324-3p*分别通过抑制基因*ATF4*、*SLC7A11*和*GPX4*的表达来促进铁死亡[21-23]。笔者推测，作为FZD7上游的调控因子miR-1-3p可能通过调控FZD7的表达影响卵巢癌细胞铁死亡。本研究首先检测并验证了FZD7是miR-1-3p的直接靶点，随后检测miR-1-3p在卵巢癌细胞系中的表达情况。结果显示：与正常卵巢上皮细胞系HOSE细胞相比，人卵巢癌细胞系HO8910或SKOV3细胞中miR-1-3p的表达均显著下调。且研究发现：在胃癌[24]、肾细胞癌[25]、膀胱癌[26]等肿瘤中，miR-1-3p均抑制肿瘤的发展。因此，我们推测在卵巢癌中，miR-1-3p也是抑癌因子。本研究进一步观察了miR-1-3p对Erastin或RSL3诱导的铁死亡的影响，结果显示：miR-1-3p增强了人卵巢癌细胞系HO8910和SKOV3对Erastin或RSL3诱导的铁死亡的敏感性。为了进一步探究miR-1-3p是否通过靶向FZD7参与卵巢癌铁死亡，我们采用Erastin或RSL3处理经FZD7过表达慢病毒感染和转染miR-1-3p模拟物的HO8910或SKOV3细胞，结果显示：miR-1-3p显著增强Erastin或RSL3诱导的细胞死亡并使细胞内MDA的水平升高，但这种增强作用可以被FZD7的过表达所取消。

本研究也存在不足。首先，未收集到卵巢癌组织样本，因此无法检测miR-1-3p在卵巢组织中的表达；其次，只探究了FZD7的上游分子机制，而未探究FZD7抑制卵巢癌细胞铁死亡的下游分子机制。

综上所述，本研究发现，在卵巢癌细胞中，miR-1-3p通过抑制FZD7的表达来增强卵巢癌细胞对Erastin或RSL3诱导铁死亡的敏感性。

作者贡献声明：章迪 论文撰写；屈斌 实验操作，论文构想；胡彬、曹可欣 数据统计和分析；沈浩明 论文指导和审阅。所有作者阅读并同意最终的文本。

利益冲突声明：作者声称无任何利益冲突。

参考文献

[1] Moghadam ER, Ang HL, Asnaf SE, et al. Broad-spectrum preclinical antitumor activity of chrysin: current trends and future perspectives[J]. Biomolecules, 2020, 10(10): 1374. https://doi.org/10.3390/biom10101374.

[2] Siegel RL, Miller KD, Jemal A. Cancer statistics, 2019[J]. CA Cancer J Clin, 2019, 69(1): 7-34. https://doi. org/10.3322/caac.21551.

[3] Zhang M, Cheng S, Jin Y, et al. Roles of CA125 in diagnosis, prediction, and oncogenesis of ovarian cancer[J]. Biochim Biophys Acta Rev Cancer, 2021, 1875(2): 188503. https://doi.org/10.1016/j.bbcan.2021.188503.

[4] Flanagan DJ, Barker N, Costanzo NSD, et al. Frizzled-7 is required for Wnt signaling in gastric tumors with and without *Apc* mutations[J]. Cancer Res, 2019, 79(5): 970-981. https://doi.org/10.1158/0008-5472.CAN-18-2095.

[5] Pi J, Wang W, Ji M, et al. YTHDF1 promotes gastric carcinogenesis by controlling translation of *FZD7*[J]. Cancer Res, 2021, 81(10): 2651-2665. https://doi. org/10.1158/0008-5472.CAN-20-0066.

[6] Wu D, Zhu J, Fu Y, et al. LncRNA HOTAIR promotes breast cancer progression through regulating the miR-129-5p/FZD7 axis[J]. Cancer Biomark, 2021, 30(2): 203-212. https://doi.org/10.3233/CBM-190913.

[7] Do M, Wu CCN, Sonavane PR, et al. A FZD7-specific

antibody-drug conjugate induces ovarian tumor regression in preclinical models[J]. Mol Cancer Ther, 2022, 21(1): 113-124. https://doi.org/10.1158/1535-7163.MCT-21-0548.

[8] Tan M, Asad M, Heong V, et al. The FZD7-TWIST1 axis is responsible for anoikis resistance and tumorigenesis in ovarian carcinoma[J]. Mol Oncol, 2019, 13(4): 757-780. https://doi.org/10.1002/1878-0261.12425.

[9] Wang Y, Zhao G, Condello S, et al. Frizzled-7 identifies platinum-tolerant ovarian cancer cells susceptible to ferroptosis [J]. Cancer Res, 2021, 81(2): 384-399. https://doi.org/10.1158/0008-5472.CAN-20-1488.

[10] Jiang X, Stockwell BR, Conrad M. Ferroptosis: mechanisms, biology and role in disease[J]. Nat Rev Mol Cell Biol, 2021, 22 (4): 266-282. https://doi.org/10.1038/s41580-020-00324-8.

[11] Carbone M, Melino G. Stearoyl CoA desaturase regulates ferroptosis in ovarian cancer offering new therapeutic perspectives[J]. Cancer Res, 2019, 79(20): 5149-5150. https://doi.org/10.1158/0008-5472.CAN-19-2453.

[12] Zhang Y, Xia M, Zhou Z, et al. p53 promoted ferroptosis in ovarian cancer cells treated with human serum incubated-superparamagnetic iron oxides[J]. Int J Nanomedicine, 2021, 16: 283-296. https://doi.org/10.2147/IJN.S282489.

[13] Stockwell BR, Friedmann Angeli JP, Bayir H, et al. Ferroptosis: a regulated cell death nexus linking metabolism, redox biology, and disease[J]. Cell, 2017, 171(2): 273-285. https://doi.org/10.1016/j.cell.2017.09.021.

[14] Galluzzi L, Vitale I, Aaronson SA, et al. Molecular mechanisms of cell death: recommendations of the Nomenclature Committee on Cell Death 2018[J]. Cell Death Differ, 2018, 25(3): 486-541. https://doi. org/10.1038/s41418-017-0012-4.

[15] Wang C, Shi M, Ji J, et al. Stearoyl-CoA desaturase 1 (SCD1) facilitates the growth and anti-ferroptosis of gastric cancer cells and predicts poor prognosis of gastric cancer[J]. Aging (Albany NY), 2020, 12(15): 15374-15391. https://doi. org/10.18632/aging.103598.

[16] Liu P, Wu D, Duan J, et al. NRF_2 regulates the sensitivity of human NSCLC cells to cystine deprivation-induced ferroptosis via FOCAD-FAK signaling pathway[J/OL]. Redox Biol, 2020, 37: 101702 [2022-08-15]. https://doi. org/10.1016/j. redox. 2020.101702.

[17] Zhang Y, Fu X, Jia J, et al. Glioblastoma therapy using codelivery of cisplatin and glutathione peroxidase targeting siRNA from iron oxide nanoparticles[J]. ACS Appl Mater Interfaces, 2020, 12(39): 43408-43421. https://doi.org/10.1021/acsami.0c12042.

[18] Chan DW, Yung MM, Chan YS, et al. MAP30 protein from Momordica charantia is therapeutic and has synergic activity with cisplatin against ovarian cancer in vivo by altering metabolism and inducing ferroptosis[J]. Pharmacol Res, 2020, 161: 105157. https://doi.org/10.1016/j.phrs.2020.105157.

[19] Luo M, Wu L, Zhang K, et al. miR-137 regulates ferroptosis by targeting glutamine transporter SLC1A5 in melanoma[J]. Cell Death Differ, 2018, 25(8): 1457-1472. https://doi. org/10.1038/s41418-017-0053-8.

[20] Zhang K, Wu L, Zhang P, et al. miR-9 regulates ferroptosis by targeting glutamic-oxaloacetic transaminase GOT1 in melanoma[J]. Mol Carcinog, 2018, 57(11): 1566-1576. https://doi.org/10.1002/mc.22878.

[21] Bai T, Liang R, Zhu R, et al. MicroRNA-214-3p enhances erastin-induced ferroptosis by targeting ATF_4 in hepatoma cells [J]. J Cell Physiol, 2020, 235(7/8): 5637-5648. https://doi. org/10.1002/jcp.29496.

[22] Mao SH, Zhu CH, Nie Y, et al. Levobupivacaine induces ferroptosis by miR-489-3p/SLC7A11 signaling in gastric cancer [J]. Front Pharmacol, 2021, 12: 681338. https://doi. org/10.3389/fphar.2021.681338.

[23] Hou Y, Cai S, Yu S, et al. Metformin induces ferroptosis by targeting miR-324-3p/GPX4 axis in breast cancer[J]. Acta Biochim Biophys Sin (Shanghai), 2021, 53(3): 333-341. https://doi.org/10.1093/abbs/gmaa180.

[24] Ke J, Zhang BH, Li YY, et al. MiR-1-3p suppresses cell proliferation and invasion and targets STC2 in gastric cancer [J]. Eur Rev Med Pharmacol Sci, 2019, 23(20): 8870-8877. https://doi.org/10.26355/eurrev_201910_19282.

[25] Liu J, Huang Y, Cheng Q, et al. miR-1-3p suppresses the epithelial-mesenchymal transition property in renal cell cancer by downregulating Fibronectin 1[J]. Cancer Manag Res, 2019, 11: 5573-5587. https://doi.org/10.2147/CMAR.S200707.

[26] Gao L, Yan P, Guo FF, et al. MiR-1-3p inhibits cell proliferation and invasion by regulating BDNF-TrkB signaling pathway in bladder cancer[J]. Neoplasma, 2018, 65(1): 89-96. https://doi.org/10.4149/neo_2018_161128N594.

（本文编辑　宋柳，郭征）

本文引用：章迪, 屈斌, 胡彬, 曹可欣, 沈浩明. MiR-1-3p通过靶向FZD7增强卵巢癌细胞对铁死亡的敏感性[J]. 中南大学学报(医学版), 2022, 47(11): 1512-1521. DOI: 10.11817/j. issn. 1672-7347.2022.210800

Cite this article as: ZHANG Di, QU Bin, HU Bin, CAO Kexin, SHEN Haoming. MiR-1-3p enhances the sensitivity of ovarian cancer cells to ferroptosis by targeting FZD7[J]. Journal of Central South University. Medical Science, 2022, 47(11): 1512-1521. DOI: 10.11817/j.issn.1672-7347.2022.210800